Robotica (2016) volume 34, pp. 2669–2688. © Cambridge University Press 2015
doi:10.1017/S0263574715000284

Dual arm-angle parameterisation and its applications for analytical inverse kinematics of redundant manipulators

Wenfu Xu†,‡* Lei Yan†,‡, Zonggao Mu†,§ and Zhiying Wang†

†*Shenzhen Graduate School, Harbin Institute of Technology, Shenzhen, P. R. China*
‡*Shenzhen Engineering Laboratory of Digital Stage Performance Robot, Shenzhen, P. R. China*
§*Aerospace Dongfanghong Development Ltd, Shenzhen, P. R. China*

(Accepted March 27, 2015. First published online: April 29, 2015)

SUMMARY

An S-R-S (Spherical-Revolute-Spherical) redundant manipulator is similar to a human arm and is often used to perform dexterous tasks. To solve the inverse kinematics analytically, the arm-angle was usually used to parameterise the self-motion. However, the previous studies have had shortcomings; some methods cannot avoid algorithm singularity and some are unsuitable for configuration control because they use a temporary reference plane. In this paper, we propose a method of analytical inverse kinematics resolution based on dual arm-angle parameterisation. By making use of two orthogonal vectors to define two absolute reference planes, we obtain two arm angles that satisfy a specific condition. The algorithm singularity problem is avoided because there is always at least one arm angle to represent the redundancy. The dual arm angle method overcomes the shortcomings of traditional methods and retains the advantages of the arm angle. Another contribution of this paper is the derivation of the absolute reference attitude matrix, which is the key to the resolution of analytical inverse kinematics but has not been previously addressed. The simulation results for typical cases that include the algorithm singularity condition verified our method.

KEYWORDS: Redundant manipulators; Analytical inverse kinematics; Arm-angle parameterisation; Algorithm singularity; Redundancy resolution.

1. Introduction

A redundant seven-degrees-of-freedom (DOF) manipulator has great advantages over a non-redundant six-DOF manipulator in obstacle avoidance,[1] joint torque optimisation,[2] failure-tolerant control,[3,4] singularity handling[5] and other factors.[6] The redundancy can also be used to minimise the reaction torque for a space manipulator.[7] Generally, the methods of kinematic redundancy resolution can be placed into two categories: methods that specify secondary tasks and methods that optimise some performance indices.[8,9] The well-known manipulators that have been launched to the international space station, including the Special Purpose Dexterous Manipulator,[10] the European Robotic Arm[11] and the Space Station Remote Manipulator System (also called Candarm2[12]), are all seven-DOF serial manipulators. The Lightweight Robot[13] designed by the DLR (German Aerospace Center) is also a redundant manipulator.

A commonly used class of redundant manipulators has joints that are arranged to form a shoulder, elbow and wrist. The shoulder joints (joints 1 through 3) and wrist joints (5 through 7) can be regarded as virtual spherical joints because the three consecutive joint axes intersect at a single

* Corresponding author. E-mail: wfxu@hit.edu.cn

point. Moreover, any two adjacent joint axes are perpendicular. S-R-S structures[14] such as the DLR Lightweight Robot[13] are similar to human arms. Soechting[15] and Liu and Todorov[16] studied the modelling and control of human arm movement in manipulator kinematics and dynamics. To supply the basis for the trajectory planning and motion control of this class of redundant manipulators, the inverse kinematics problem must be solved.

In contrast to a six-DOF manipulator, a redundant manipulator has infinite configurations for a given end-effector pose (position and attitude). Therefore, a parameter must be defined to describe the redundancy. Lee and Bejczy[17] proposed a joint parameterisation method, but the selection of an appropriate joint is difficult. Moradi and Lee[18] defined the redundancy circle and used a position on the circle as the redundancy parameter. Based on the description of the human arm's posture, Asfour and Dillmann[19] analytically solved the inverse kinematics of a humanoid robot arm. Tondu[20] used the shoulder abduction angle (i.e., θ_1 for the given manipulator) as the redundancy parameter and derived the closed-form inverse kinematics for an anthropomorphic arm. The above methods can be classified as joint parameterisation approaches or Cartesian space self-motion parameterisation methods. For the former, a certain joint displacement is itself regarded as the redundancy parameter. The selection of the angle for the parameterisation is difficult. It cannot uniquely represent the redundancy of the manipulator. In contrast, self-motion parameterisation is specialised to a specific arm and seems to be unsuitable for S-R-S manipulators.[21]

The arm angle proposed by Kreutz-Delgado[22] is a better parameter for describing the self-motion of a generic anthropomorphic manipulator. It specifies the unique elbow position for a given hand pose. However, algorithm singularity exists when the fixed vector used to define the reference plane and the axis connecting the shoulder and wrist are collinear, which means that the reference plane is indeterminate. To handle this problem, Shimizu[21] used a temporary arm plane to define the arm angle. They constructed a virtual non-redundant manipulator by setting the value of θ_3 to 0. The arm plane formed by the virtual non-redundant manipulator was considered to be the reference plane. It is possible to avoid algorithm singularity. However, each specified pose has eight solutions for the virtual non-redundant manipulator; the arm plane is not unique. The eight solutions determine four potential arm planes (see Section 3). As the reference plane is not absolute, it is not suitable for configuration control.

In this paper, we propose an analytical inverse kinematics resolution method based on dual arm-angle parameterisation that overcomes shortcomings such as algorithm singularity and a temporary reference plane while retaining the advantages of arm-angle parameterisation. The dual arm angle is an extension of the arm angle. Two orthogonal vectors are selected as reference vectors to define two reference planes. Two arm angles, which are the angles between the arm plane and the two reference planes, are obtained. These two arm angles satisfy a specific constraint condition, so they are called a "dual arm angle". Because the wrist point cannot lie on the two reference vectors at the same time, there is always a reasonable reference plane and a corresponding arm angle that can be used as the redundancy parameter. Therefore, the algorithm singularity problem is avoided. Another contribution of this study is the derivation of the absolute reference elbow attitude matrix ${}^0\boldsymbol{R}_3^{\psi=0}$ (the ${}^0\boldsymbol{R}_3^0$ in ref. [21] is a relative reference attitude gained by setting $\theta_3 = 0$; here ${}^0\boldsymbol{R}_3^{\psi=0}$ is the absolute reference attitude), which is the key to the resolution of analytical inverse kinematics but was not addressed in our previous paper.[21]

2. Modelling of S-R-S Redundant Manipulators

The joint layout of an S-R-S redundant manipulator is shown in Fig. 1. For some applications, such as space construction, an additional link offset can be added to the elbow to increase the range of movement. A more general model is used to describe a class of redundant manipulators with similar joint structure. The D–H frames are shown in Fig. 2, and their parameters are listed in Table I. The simplest case, $d_4 = 0$, is very similar to a human arm. For a practical example, the following parameters are used in this paper:

$$d_1 = d_7 = 0.3, d_2 = d_6 = 0.0, d_3 = d_5 = 0.7,\ d_4 = -0.3. \tag{1}$$

https://doi.org/10.1017/S0263574715000284 Published online by Cambridge University Press

Table I. D–H parameters of the S-R-S manipulator with an offset elbow.

link i	$\theta_i(^\circ)$	$\alpha_i(^\circ)$	a_i(m)	d_i(m)
1	−90	90	0	$d_1 = 0.3$
2	180	90	0	0
3	0	−90	0	$d_3 = 0.7$
4	0	90	0	$d_4 = -0.3$
5	0	−90	0	$d_5 = 0.7$
6	0	90	0	0
7	−90	0	0	$d_7 = 0.3$

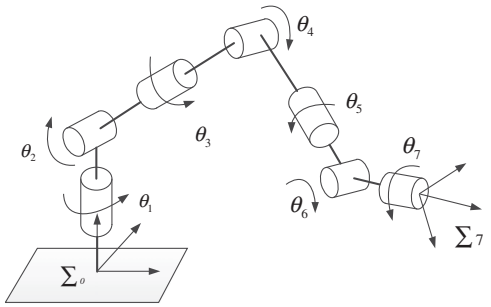

Fig. 1. Joint layout of the S-R-S redundant manipulator.

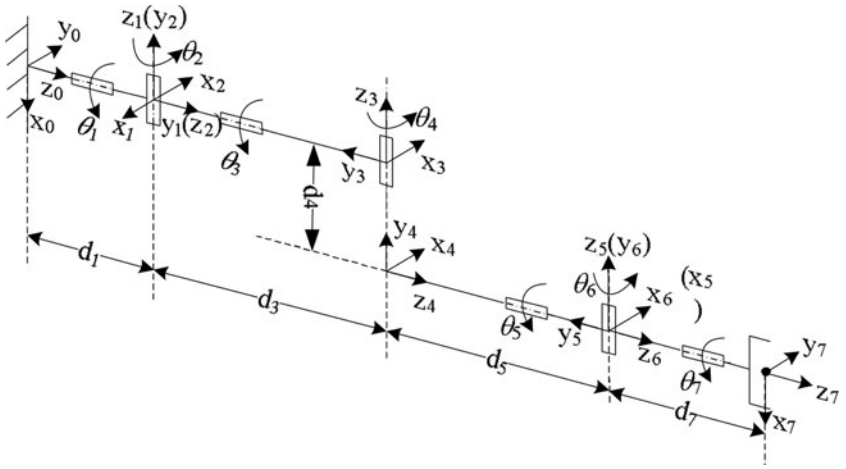

Fig. 2. D–H frames of the S-R-S manipulator with an offset elbow.

Based on the D–H notation, the homogeneous transformation matrix ${}^{i-1}\boldsymbol{T}_i$ between adjacent frames can be given as follows:

$$ {}^{i-1}\boldsymbol{T}_i = \begin{bmatrix} {}^{i-1}\boldsymbol{R}_i & {}^{i-1}\boldsymbol{P}_i \\ 0 & 1 \end{bmatrix} = \begin{bmatrix} c_{\theta_i} & -s_{\theta_i} c_{\alpha_i} & s_{\theta_i} s_{\alpha_i} & a_i c_{\theta_i} \\ s_{\theta_i} & c_{\theta_i} c_{\alpha_i} & -c_{\theta_i} s_{\alpha_i} & a_i s_{\theta_i} \\ 0 & s_{\alpha_i} & c_{\alpha_i} & d_i \\ 0 & 0 & 0 & 1 \end{bmatrix}, \tag{2} $$

where θ_i is the ith joint angle, ${}^{i-1}\boldsymbol{R}_i$ denotes the orientation of the ith frame relative to the $(i-1)$th frame and ${}^{i-1}\boldsymbol{P}_i$ is the position vector of the ith frame's origin, expressed in the $(i-1)$th frame. Moreover,

$$ \begin{cases} s_{\theta_i} = \sin(\theta_i), \mathrm{c}_{\theta_i} = \cos(\theta_i) \\ s_{\alpha_i} = \sin(\alpha_i), \mathrm{c}_{\alpha_i} = \cos(\alpha_i) \end{cases}. \tag{3} $$

https://doi.org/10.1017/S0263574715000284 Published online by Cambridge University Press

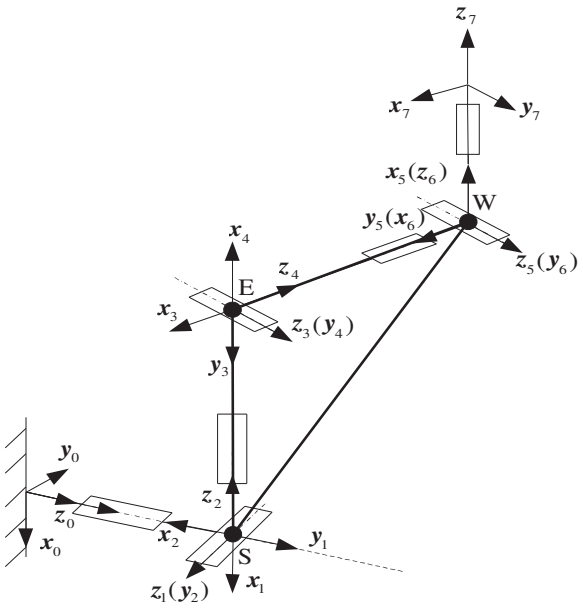

Fig. 3. Definition of the arm plane.

The pose (orientation and position) of the end-effector frame (i.e., the seventh frame 7) with respect to the base frame (frame 0) can be expressed as:

$$ {}^0\boldsymbol{T}_7 = {}^0\boldsymbol{T}_1 {}^1\boldsymbol{T}_2 \cdots {}^6\boldsymbol{T}_7 = \text{fkine}(\Theta) = \begin{bmatrix} {}^0\boldsymbol{R}_7 & {}^0\boldsymbol{P}_7 \\ 0 & 1 \end{bmatrix}, \tag{4} $$

where Θ is a column vector composed by the $\theta_1 \sim \theta_7$, fkine() is the forwards kinematics function, ${}^0\boldsymbol{R}_7$ is the attitude transformation matrix and ${}^0\boldsymbol{P}_7$ is the position vector of the end-effector with respect to the base frame, Frame 0.

For practical applications, the joint angles should be determined for control when ${}^0\boldsymbol{T}_7$ is given. The solution is expressed as:

$$ \Theta = \text{ikine}\left({}^0\boldsymbol{T}_7\right), \tag{5} $$

where ikine() is the inverse kinematics function. This paper will derive the analytical expressions for Eq. (5).

3. Arm-Angle Parameterisation Method

3.1. Arm plane and arm angle

According to the characteristics of an S-R-S manipulator, the three-axis joints of the shoulder (joints 1 through 3) and the wrist (joints 5 through 7) intersect at one point and form the equivalent of a spherical joint. The intersection points are denoted by S and W, respectively. In addition, the origin of the 3rd frame, located on the elbow (joint 4), is denoted by E. As shown in Fig. 3, the plane SEW is then defined as the arm plane.[22] The special case in which S, E and W are collinear is not considered in this paper.

Given a reference plane, the angle between the reference plane and the arm plane is defined as the arm angle ψ, which is used to represent the self-motion. We can simplify the kinematic analysis and configuration control for various purposes by choosing any plane of interest as the reference plane. Without loss of generality, the line SW is used as one line on the reference plane; only one more point (denoted as Q) not on the line is then needed to determine the reference plane, which is represented as SQW. The relationship between the reference plane, arm plane and arm angle is shown in Fig. 4. For the convenience of discussion, we define some vectors as follows:

https://doi.org/10.1017/S0263574715000284 Published online by Cambridge University Press

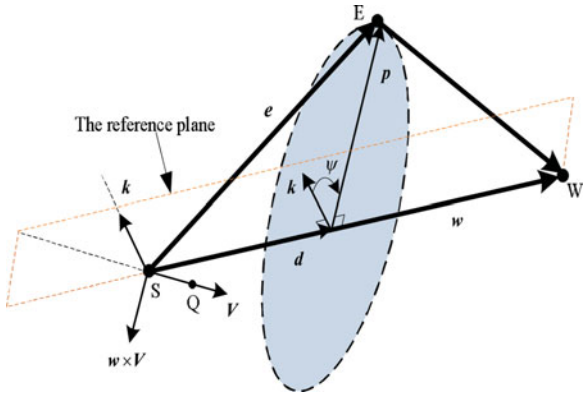

Fig. 4. Definition of the arm angle.

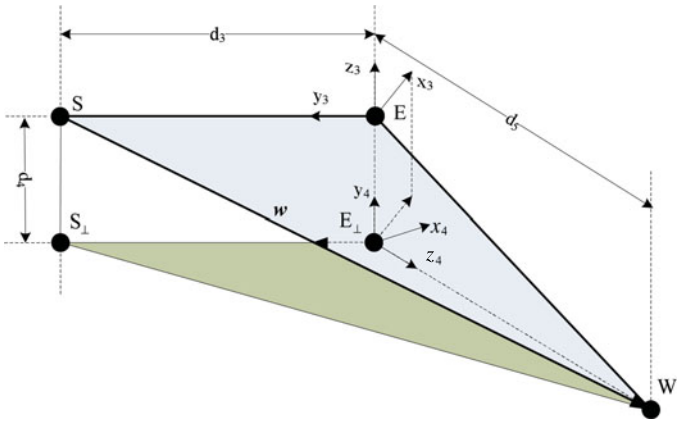

Fig. 5. Projection of the arm plane SEW.

$\boldsymbol{w}$: A vector from point S to point W;

$\boldsymbol{e}$: A vector from point S to point E;

$\boldsymbol{V}$: The vector from point S to point Q in the reference plane;

$\boldsymbol{k}$, $\boldsymbol{p}$: The vectors that are perpendicular to $\boldsymbol{w}$ in the reference plane SQW and the arm plane SEW, respectively.

$\boldsymbol{n}_i, \boldsymbol{o}_i, \boldsymbol{a}_i$ $(i = 0, 1, \cdots, 7)$: The unit vectors of the x-, y- and z-axes of the ith frame, x_i, y_i, and z_i;

$\boldsymbol{P}_i$ $(i = 0, 1, \ldots, 7)$: The position vector of the origin of the ith frame.

If a vector is described in the jth $(j = 0, 1, \ldots, 7)$ frame, the superscript "j" will be used. For example, ${}^0\boldsymbol{w}$ shows that the vector $\boldsymbol{w}$ is described in frame 0.

According to the configuration of the SRS manipulators (see Fig. 2), the vector ${}^0\boldsymbol{w}$ can be determined according to the end-effector's pose ${}^0\boldsymbol{T}_7$, i.e.,

$$ {}^0\boldsymbol{w} = {}^0\boldsymbol{P}_7 - \begin{bmatrix} 0 & 0 & d_1 \end{bmatrix}^{\mathrm{T}} - {}^0\boldsymbol{R}_7 \begin{bmatrix} 0 & 0 & d_7 \end{bmatrix}^{\mathrm{T}}. \tag{6} $$

3.2. Resolutions of joint angles

3.2.1. Determination of the elbow joint angle. To separate the elbow joint angle, we project the arm plane to the plane perpendicular to the axis of joint 4. The projected plane is denoted as $\mathrm{S}_\perp\mathrm{E}_\perp\mathrm{W}$ (see Fig. 5), and the lengths of the projected links are $S_\perp E_\perp = d_3$, $E_\perp W = d_5$. According to the Pythagorean theorem, we know that $S_\perp W^2 = |\boldsymbol{w}|^2 - d_4^2$.

https://doi.org/10.1017/S0263574715000284 Published online by Cambridge University Press

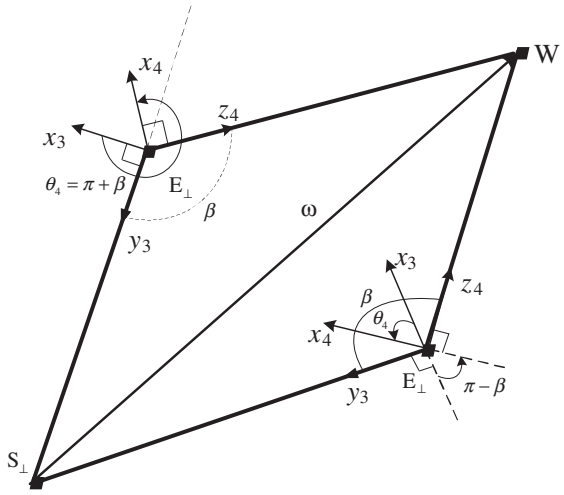

Fig. 6. Two solutions of the elbow joint angle.

Using the cosine law for the triangle $S_\perp E_\perp W$, we have

$$\beta = \operatorname{acos}\left(\frac{S_\perp E_\perp^2 + E_\perp W^2 - S_\perp W^2}{2S_\perp E \cdot E_\perp W}\right) = \operatorname{acos}\left(\frac{d_3^2 + d_5^2 + d_4^2 - |\boldsymbol{w}|^2}{2d_3 d_5}\right). \tag{7}$$

There are two cases for resolving θ_4, which is shown in Fig. 6. For the first case,

$$\theta_4 = \frac{\pi}{2} + \beta + \frac{\pi}{2} = \pi + \beta. \tag{8}$$

For the second case,

$$\theta_4 = 2\pi - \left(\frac{\pi}{2} + \beta + \frac{\pi}{2}\right) = \pi - \beta. \tag{9}$$

It can be seen that the elbow joint angle is independent of the arm angle. Given the pose of the end-effector, we can obtain two resolutions for θ_4 as follow:

$$\theta_4 = \pi \pm \beta = \pi \pm \operatorname{acos}\left(\frac{d_3^2 + d_5^2 + d_4^2 - |\boldsymbol{w}|^2}{2d_3 d_5}\right). \tag{10}$$

3.2.2. Determination of the shoulder joint angles. Given the arm-angle ψ, the transformation matrix that represents the rotation of angle ψ about the vector $\boldsymbol{w}$ is as follow:

$${}^0\boldsymbol{R}_\psi = \boldsymbol{I}_3 + \left[{}^0\boldsymbol{w}^\times\right] \sin\psi + \left[{}^0\boldsymbol{w}^\times\right]^2 (1 - \cos\psi), \tag{11}$$

where the left superscript "0" indicates the reference frame, $\boldsymbol{I}_3$ is a 3×3 identity matrix and ${}^0\boldsymbol{w}^\times$ is the skew symmetric matrix of ${}^0\boldsymbol{w}$,

$$\text{for} \quad {}^0\boldsymbol{w} = \begin{bmatrix} w_1 \\ w_2 \\ w_3 \end{bmatrix}, \quad {}^0\boldsymbol{w}^\times = \begin{pmatrix} 0 & -w_3 & w_2 \\ w_3 & 0 & -w_1 \\ -w_2 & w_1 & 0 \end{pmatrix}. \tag{12}$$

https://doi.org/10.1017/S0263574715000284 Published online by Cambridge University Press

When $\psi = 0$, the orientation of frame 3 relative to frame 0 is denoted by ${}^0\boldsymbol{R}_3^{\psi=0}$ and is called the shoulder reference attitude matrix. For a given value of ψ, the orientation of the frame 3 relative to frame 0 can be calculated as follows:

$$ {}^0\boldsymbol{R}_3 = {}^0\boldsymbol{R}_\psi \, {}^0\boldsymbol{R}_3^{\psi=0}. \tag{13} $$

Substituting Eq. (11) into Eq. (13) yields

$$ {}^0\boldsymbol{R}_3 = \boldsymbol{A}_s \sin\psi + \boldsymbol{B}_s \cos\psi + \boldsymbol{C}_s = \begin{bmatrix} r_{11} & r_{12} & r_{13} \\ r_{21} & r_{22} & r_{23} \\ r_{31} & r_{32} & r_{33} \end{bmatrix}, \tag{14} $$

where $\boldsymbol{A}_s = \left[{}^0\boldsymbol{w}^\times\right] {}^0\boldsymbol{R}_3^{\psi=0}$, $\boldsymbol{B}_s = -\left[{}^0\boldsymbol{w}^\times\right]^2 {}^0\boldsymbol{R}_3^{\psi=0}$ and $\boldsymbol{C}_s = \left(\boldsymbol{I}_3 + \left[{}^0\boldsymbol{w}^\times\right]^2\right) {}^0\boldsymbol{R}_3^{\psi=0}$. If a_{sij} and b_{sij}, respectively, represent the element of the ith row and jth of the matrix $\boldsymbol{A}_s$ and $\boldsymbol{B}_s$, the (i, j) element of ${}^0\boldsymbol{R}_3$ can be calculated as follows according to Eq. (14)

$$ r_{ij} = a_{sij}\mathrm{s}_\psi + b_{sij}\mathrm{c}_\psi + c_{sij}, \tag{15} $$

where $s_\psi = \sin\psi$, $c_\psi = \cos\psi$. From the definition of the rotation matrix, we have

$$ {}^0\boldsymbol{R}_3 = {}^0\boldsymbol{R}_1 \, {}^1\boldsymbol{R}_2 \, {}^2\boldsymbol{R}_3 = \begin{bmatrix} s_1 s_3 + c_1 c_2 c_3 & -c_1 s_2 & s_1 c_3 - c_1 c_2 s_3 \\ -c_1 s_3 + s_1 c_2 c_3 & -s_1 s_2 & -c_1 c_3 - s_1 c_2 s_3 \\ c_3 s_2 & c_2 & -s_2 s_3 \end{bmatrix}. \tag{16} $$

Combining Eqs. (14) and (16), the following result is obtained:

$$ \begin{bmatrix} r_{11} & r_{12} & r_{13} \\ r_{21} & r_{22} & r_{23} \\ r_{31} & r_{32} & r_{33} \end{bmatrix} = \begin{bmatrix} s_1 s_3 + c_1 c_2 c_3 & -c_1 s_2 & s_1 c_3 - c_1 c_2 s_3 \\ -c_1 s_3 + s_1 c_2 c_3 & -s_1 s_2 & -c_1 c_3 - s_1 c_2 s_3 \\ c_3 s_2 & c_2 & -s_2 s_3 \end{bmatrix}. \tag{17} $$

Comparing the elements from (1, 2) and (2, 2),

$$ s_2 = \sqrt{r_{12}^2 + r_{22}^2} \quad \text{or} \quad s_2 = -\sqrt{r_{12}^2 + r_{22}^2}. \tag{18} $$

We can then obtain two solutions for θ_2 combing Eqs. (17) and (18):

$$ \theta_2 = \operatorname{atan2}\left(\sqrt{r_{12}^2 + r_{22}^2}, r_{32}\right) \quad \text{or} \quad \theta_2 = \operatorname{atan2}\left(-\sqrt{r_{12}^2 + r_{22}^2}, r_{32}\right). \tag{19} $$

Based on the calculated value for θ_2, the following results are obtained:

$$ \begin{cases} s_1 = -\left(a_{s22}\mathrm{s}_\psi + b_{s22}\mathrm{c}_\psi + c_{s22}\right)/s_2 \\ c_1 = -\left(a_{s12}\mathrm{s}_\psi + b_{s12}\mathrm{c}_\psi + c_{s12}\right)/s_2 \end{cases}, \tag{20} $$

$$ \begin{cases} s_3 = -\left(a_{s33}\mathrm{s}_\psi + b_{s33}\mathrm{c}_\psi + c_{s33}\right)/s_2 \\ c_3 = \left(a_{s31}\mathrm{s}_\psi + b_{s31}\mathrm{c}_\psi + c_{s31}\right)/s_2 \end{cases}. \tag{21} $$

According to Eqs. (20) and (21), we can solve θ_2 and θ_3 using the "atan2()" function. To avoid the numerical problems caused by $s_2 \approx 0$, the following equations are used:

$$ \begin{cases} \theta_1 = \operatorname{atan2}\left(-\left(a_{s22}\mathrm{s}_\psi + b_{s22}\mathrm{c}_\psi + c_{s22}\right) s_2, \right. \\ \qquad\qquad \left. -\left(a_{s12}\mathrm{s}_\psi + b_{s12}\mathrm{c}_\psi + c_{s12}\right) s_2\right) \\ \theta_3 = \operatorname{atan2}\left(-\left(a_{s33}\mathrm{s}_\psi + b_{s33}\mathrm{c}_\psi + c_{s33}\right) s_2, \right. \\ \qquad\qquad \left. \left(a_{s31}\mathrm{s}_\psi + b_{s31}\mathrm{c}_\psi + c_{s31}\right) s_2\right) \end{cases}. \tag{22} $$

https://doi.org/10.1017/S0263574715000284 Published online by Cambridge University Press

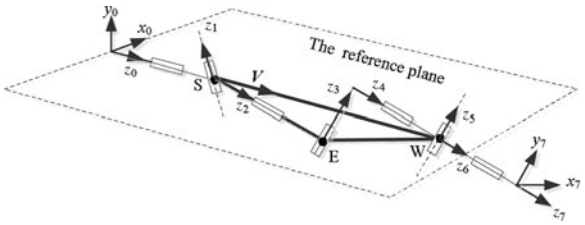

Fig. 7. Algorithm singularity of the S-R-S manipulator.

3.2.3. Determination of the wrist joint angles. The attitude rotation matrix from frame 3 to frame 4 is

$$ {}^{3}\boldsymbol{R}_4 = \begin{bmatrix} c_{\theta_4} & -c_{\alpha_4}s_{\theta_4} & s_{\alpha_4}s_{\theta_4} \\ s_{\theta_4} & c_{\alpha_4}c_{\theta_4} & -s_{\alpha_4}c_{\theta_4} \\ 0 & s_{\alpha_4} & c_{\alpha_4} \end{bmatrix} = \begin{bmatrix} c_4 & 0 & s_4 \\ s_4 & 0 & -c_4 \\ 0 & 1 & 0 \end{bmatrix}. \tag{23} $$

The attitude of frame 4 with respect to frame 7 is given by the following:

$$ {}^{7}\boldsymbol{R}_4 = {}^{0}\boldsymbol{R}_7^{T}\,{}^{0}\boldsymbol{R}_{\psi}\left({}^{0}\boldsymbol{R}_3^{\psi=0}\right)\left({}^{3}\boldsymbol{R}_4\right) = \boldsymbol{A}_w \sin\psi + \boldsymbol{B}_w \cos\psi + \boldsymbol{C}_w, \tag{24} $$

where $\boldsymbol{A}_w = {}^{0}\boldsymbol{R}_7^{T}\left[{}^{0}\boldsymbol{w}^{\times}\right]{}^{0}\boldsymbol{R}_3^{\psi=0}\left({}^{3}\boldsymbol{R}_4\right)$, $\boldsymbol{B}_w = -{}^{0}\boldsymbol{R}_7^{T}\left[{}^{0}\boldsymbol{w}^{\times}\right]^2{}^{0}\boldsymbol{R}_3^{\psi=0}\left({}^{3}\boldsymbol{R}_4\right)$,

$$ \boldsymbol{C}_w = {}^{0}\boldsymbol{R}_7^{T}\left(\boldsymbol{I}_3 + \left[{}^{0}\boldsymbol{w}^{\times}\right]^2\right){}^{0}\boldsymbol{R}_3^{\psi=0}\left({}^{3}\boldsymbol{R}_4\right). $$

In contrast,

$$ {}^{7}\boldsymbol{R}_4 = \left({}^{4}\boldsymbol{R}_5\,{}^{5}\boldsymbol{R}_6\,{}^{6}\boldsymbol{R}_7\right)^{\mathrm{T}} = \begin{bmatrix} c_5c_6c_7 - s_5s_7 & -c_5c_6s_7 - s_5c_7 & c_5s_6 \\ s_5c_6c_7 + c_5s_7 & -s_5c_6s_7 + c_5c_7 & s_5s_6 \\ -s_6c_7 & s_6s_7 & c_6 \end{bmatrix}. \tag{25} $$

According to Eqs. (24) and (25), we can obtain, two groups of θ_5, θ_6 , θ_7 as follow:

$$ \begin{cases} \theta_6 = \operatorname{atan2}\left(\pm\sqrt{\left(a_{w13}\mathrm{s}_{\psi} + b_{w13}\mathrm{c}_{\psi} + c_{w13}\right)^2 + \left(a_{w23}\mathrm{s}_{\psi} + b_{w23}\mathrm{c}_{\psi} + c_{w23}\right)^2},\right. \\ \qquad\qquad \left. a_{w33}\mathrm{s}_{\psi} + b_{w33}\mathrm{c}_{\psi} + c_{w33}\right) \\ \theta_5 = \operatorname{atan2}\left(\left(a_{w23}\mathrm{s}_{\psi} + b_{w23}\mathrm{c}_{\psi} + c_{w23}\right)s_6,\right. \\ \qquad\qquad \left.\left(a_{w13}\mathrm{s}_{\psi} + b_{w13}\mathrm{c}_{\psi} + c_{w13}\right)s_6\right) \\ \theta_7 = \operatorname{atan2}\left(\left(a_{w32}\mathrm{s}_{\psi} + b_{w32}\mathrm{c}_{\psi} + c_{w32}\right)s_6,\right. \\ \qquad\qquad \left. -\left(a_{w31}\mathrm{s}_{\psi} + b_{w31}\mathrm{c}_{\psi} + c_{w31}\right)s_6\right) \end{cases}, \tag{26} $$

where a_{wij} and b_{wij} represent the element of the ith row and jth column of the matrices $\boldsymbol{A}_w$ and $\boldsymbol{B}_w$, respectively.

3.3. Existing problems for the previous methods

3.3.1. Algorithm singularity[22]. According to the definitions of the reference plane and the arm angle in Fig. 4, we notice that when the point W is located on the straight line along vector $\boldsymbol{V}$ (as shown in Fig. 7), the reference plane degenerates into a straight line. The arm-angle therefore loses its definition, and the arm-angle parameterisation method fails to solve the joint angles. This situation – algorithm singularity – is described in the literature,[22] but no feasible methods of avoiding it have been provided.

3.3.2. Only four solutions are determined for a given arm angle[21]. The resolution process of the single arm-angle parameterisation method is shown in Fig. 8.

https://doi.org/10.1017/S0263574715000284 Published online by Cambridge University Press

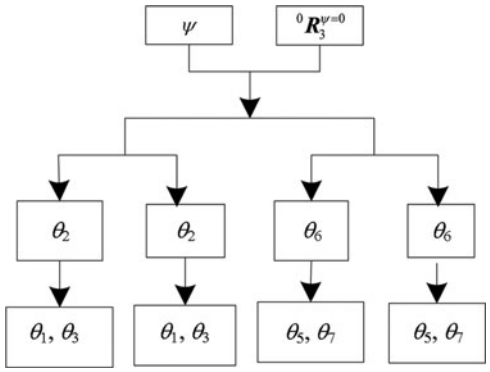

Fig. 8. Process of the original arm parameterisation method.

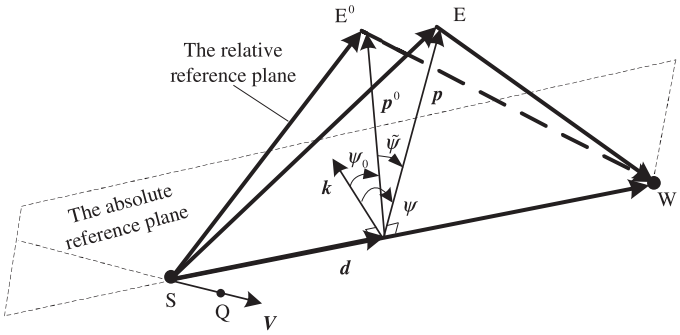

Fig. 9. Absolute arm angle and relative arm angle.

We can see that the process only provides four sets of solutions. When the redundancy parameter is selected, an S-R-S manipulator should have eight sets of solutions. That is to say, the traditional method, presented by ref. [21], cannot supply all of the solutions for the inverse kinematics.

3.3.3. Relative reference plane and relative Arm Angle[21]. To avoid the algorithm singularity problem mentioned above, Ref. [21] proposed a practical method that used a "floating" plane as the reference plane. Fixing joint 3 at the zero position, $\theta_3 = 0^\circ$, the original seven-DOF manipulator degenerates into a six-DOF manipulator with a configuration similar to that of a Programmable Universal Machine for Assembly (PUMA)-type robot. It is very easy to solve the inverse kinematics of a six-DOF manipulator. We can obtain eight sets of solutions for joints 1, 2 and 4 through 7 joints of the original manipulator. The solved joint angles corresponding to $\theta_3 = 0^\circ$ are denoted $\theta_1^0, \theta_2^0, \ldots, \theta_7^0$ The attitude of frame 3 relative to frame 0 is then calculated according to the following equation:

$$ {}^0_{\text{rel}}\boldsymbol{R}_3^0 = {}^0\boldsymbol{R}_1^{01} \cdot \boldsymbol{R}_2^{02} \cdot \boldsymbol{R}_3^0, \tag{27} $$

where the right superscript "0" of ${}^i\boldsymbol{R}_j^0$ indicates the special case that $\theta_3 = 0$. ${}^0\boldsymbol{R}_3^0$ is a relative reference attitude. In ref. [21], an arbitrary arm plane formed by any set of solutions of the case $\theta_3 = 0^\circ$ can be selected as the reference plane, which is not a definite plane corresponding to a given end-effector's pose. Hence, it is a "relative" reference plane that has multiple alternatives and is not favourable for configuration control.[23] The angle between the practical arm plane and the relative reference plane is then called the relative arm angle and is denoted by $\tilde{\psi}$.

To solve this problem, we define the absolute reference plane according to a fixed reference frame (such as $x_0y_0z_0$) and the given end-effector's pose. The angle between the practical arm plane and the absolute reference plane is taken as the absolute arm angle and is denoted by ψ. Correspondingly, the absolute reference attitude ${}^0\boldsymbol{R}_3^{\psi=0}$ will be used instead of ${}^0_{\text{rel}}\boldsymbol{R}_3^0$.

The relationships of the absolute and relative reference planes and arm angles are shown in Fig. 9, where

E^0, E: the elbow points in the relative reference plane and the practical arm plane, respectively;

https://doi.org/10.1017/S0263574715000284 Published online by Cambridge University Press

$\boldsymbol{p}^0$, p: the perpendicular vectors of line SW through E^0 and E, respectively; and

ψ_o: the angle from the absolute reference plane to the relative reference plane.

According to the definitions of the angles between two planes, we can establish the equation as follows:

$$\psi = \psi_o + \tilde{\psi}. \tag{28}$$

4. Dual Arm-Angle Parameterisation Without Algorithm Singularity

From the analysis above, some cases will occur in which point W is located on the line along the reference vector $\boldsymbol{V}$. Algorithm singularity always exists for single arm-angle parameterisation methods. Here, we propose the dual arm-angle concept and a corresponding parameterisation method to fundamentally eliminate algorithm singularity. Two vectors (denoted $\boldsymbol{V}_1$ and $\boldsymbol{V}_2$) are selected as the reference vectors, which form two reference planes with the vector $\boldsymbol{w}$. The angles between the arm plane SEW and the two reference planes are defined as the two arm angles. Because wrist point W cannot lie on two lines at the same time, there is always an effective arm angle that can be used to parameterise the self-motion. The intersection point of the two lines is wrist point S. The special case in which point W coincides with point S is not considered. The inverse kinetics equation can then be solved based on the effective arm angle.

Without loss of generality, we select two orthogonal vectors $\boldsymbol{V}_1$ and $\boldsymbol{V}_2$ as the reference vectors to simplify the calculation. Here, the z_0-axis and x_0-axis are considered to be $\boldsymbol{V}_1$ and $\boldsymbol{V}_2$, respectively. The corresponding arm angles are denoted by ψ_z and ψ_x. Because ψ_z and ψ_x are constrained by a definite relationship, they are called dual arm angles.

4.1. Dual arm-angles ψ_z and ψ_x

As mentioned above, when the reference vector $\boldsymbol{V}$ is selected, the plane formed by $\boldsymbol{V}$ and point W is the reference plane. According to Fig. 4 and previous definitions, the projection of vector $\boldsymbol{e}$ on vector $\boldsymbol{w}$ is given by

$$\boldsymbol{d} = \hat{\boldsymbol{w}} \left(\hat{\boldsymbol{w}}^{\mathrm{T}} \boldsymbol{e} \right), \tag{29}$$

where $\hat{\boldsymbol{w}}$ is the unit vector of $\boldsymbol{w}$, $\hat{\boldsymbol{w}}=\boldsymbol{w}/\|\boldsymbol{w}\|$. In this paper, $\|\cdot\|$ denotes the norm of a vector.

In the arm plane, the vector perpendicular to $\boldsymbol{w}$ is given by

$$\boldsymbol{p} = \boldsymbol{e} - \boldsymbol{d} = \left(\boldsymbol{I} - \hat{\boldsymbol{w}} \hat{\boldsymbol{w}}^{\boldsymbol{T}} \right) \boldsymbol{e}. \tag{30}$$

Its unit vector $\hat{\boldsymbol{p}}$ is

$$\hat{\boldsymbol{p}} = \frac{\boldsymbol{p}}{\|\boldsymbol{p}\|}. \tag{31}$$

In contrast, in the reference plane, the vector vertical to $\boldsymbol{w}$ is calculated as follows:

$$\boldsymbol{n} = (\boldsymbol{w} \times \boldsymbol{V}) \times \boldsymbol{w} = \boldsymbol{w} \times (\boldsymbol{w} \times \boldsymbol{V}) = \boldsymbol{w}^{\times} \boldsymbol{w}^{\times} \boldsymbol{V}. \tag{32}$$

The unit vector $\hat{\boldsymbol{n}}$ is

$$\hat{n} = \frac{\boldsymbol{n}}{\|\boldsymbol{n}\|}. \tag{33}$$

According to the properties of dot and cross products of vectors, the following results are obtained:

$$\begin{cases} c_\psi = \hat{\boldsymbol{n}}^{\boldsymbol{T}} \hat{\boldsymbol{p}} \\ s_\psi = \hat{\boldsymbol{w}}^{\boldsymbol{T}} (\hat{\boldsymbol{n}} \times \hat{\boldsymbol{p}}) = \hat{\boldsymbol{w}}^{\boldsymbol{T}} \left(\hat{\boldsymbol{n}}^{\times} \hat{\boldsymbol{p}} \right) \end{cases}. \tag{34}$$

Therefore,

$$\psi = \operatorname{atan2}\left(s_\psi, c_\psi \right) = \operatorname{atan2}\left(\hat{\boldsymbol{w}}^{\boldsymbol{T}} \left(\boldsymbol{V}^{\times} \boldsymbol{p} \right), \boldsymbol{V}^{\boldsymbol{T}} \boldsymbol{p} \right). \tag{35}$$

https://doi.org/10.1017/S0263574715000284 Published online by Cambridge University Press

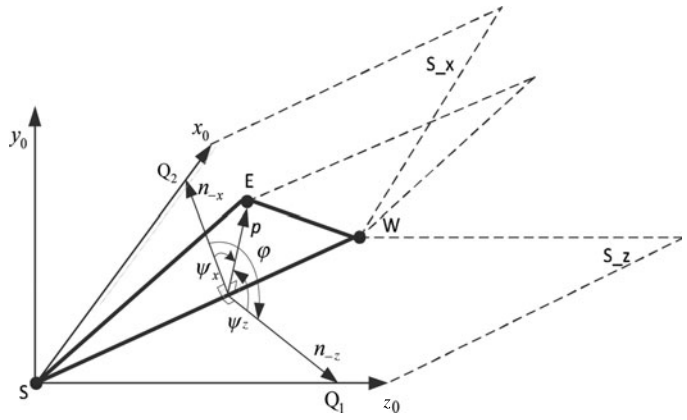

Fig. 10. Relationship between the arm angles.

Given the reference vector $\boldsymbol{V}$, the corresponding arm angle can be calculated using Eq. (35).

To determine the dual arm angles, the z_0-axis and the x_0-axis are selected to form two reference planes, denoted S_z (SQ_1W) and S_x (SQ_2W), respectively. If the z_0-axis is chosen as the reference axis, $\boldsymbol{V}={}^0\boldsymbol{a}_0 = \begin{bmatrix}0 & 0 & 1\end{bmatrix}^{\mathrm{T}}$, then ψ_z can be calculated according to Eq. (35). Substituting $\boldsymbol{V}={}^0\boldsymbol{n}_0 = \begin{bmatrix}1 & 0 & 0\end{bmatrix}^{\mathrm{T}}$ for Eq. (35), ψ_x is determined. The concept of the dual arm angle is shown in Fig. 10.

4.2. Relationship of ψ_z and ψ_x

The vector $\boldsymbol{w}$ is known when the pose of the end-effector is given. As shown in Fig. 10, the vectors $\boldsymbol{n}_{\_x}$ and $\boldsymbol{n}_{\_z}$, respectively in the reference planes S_x and S_z, are both perpendicular to line SW. The angle between the two reference planes (SQ_1W and SQ_2W), denoted φ, is determined by the two vectors $\boldsymbol{n}_{\_x}$ and $\boldsymbol{n}_{\_z}$. Its value is constant for a given end-effector pose. According to the geometry shown in Fig. 10, the following relationship exists:

$$\psi_x = \psi_z + \varphi. \tag{36}$$

For one of the arm angles, such as ψ_z, we can use the following scalar to judge whether the algorithm singularity occurs:

$$k_s = |\boldsymbol{w} \times \boldsymbol{V}|, \tag{37}$$

where the value of k_s reflects the coincident degree. $k_s = 0$ shows that the algorithm singularity occurs with a single arm angle. The other arm angle should then be used to parameterise the redundancy for solving the inverse kinematics. If the algorithm is realised using a programming language, $k_s \leq 1.00\text{E}{-}6$ can be considered equal to zero.

4.3. Analytical inverse kinematics resolution

For a given end-effector's pose, denoted by the homogeneous matrix ${}^0\boldsymbol{T}_7$, the analytical inverse kinematics resolution process based on the dual arm angle is shown in Figs. 11 and 12. The details of the reference vector and arm angle (see Fig. 11) are as follows:

a) Choose the default reference vector $\boldsymbol{V}$ and give a desired corresponding arm angle ψ. In this paper, the z_0-axis of the base frame, frame 0, is the default reference vector. Then $\boldsymbol{V}={}^0\boldsymbol{a}_0$, and ψ is actually ψ_z;
b) Calculate the singularity condition parameter k_s according to Eq. (37) and $\boldsymbol{V}$, and the given end-effector pose ${}^0\boldsymbol{T}_7$;
c) If $k_s \geq 1.00\text{E}{-}6$, then algorithm singularity does not exist for ψ_z, $\boldsymbol{V}={}^0\boldsymbol{a}_0$ and $\psi = \psi_z$; go to (f). Otherwise, go to (d);
d) Choose $\boldsymbol{V}={}^0\boldsymbol{n}_0$ (the unit vector of x_0-axis), and take S_z = S_x, i.e., $\varphi = 0$;
e) Calculate ψ_x according to Eq. (36), and set $\psi = \psi_x$.

https://doi.org/10.1017/S0263574715000284 Published online by Cambridge University Press

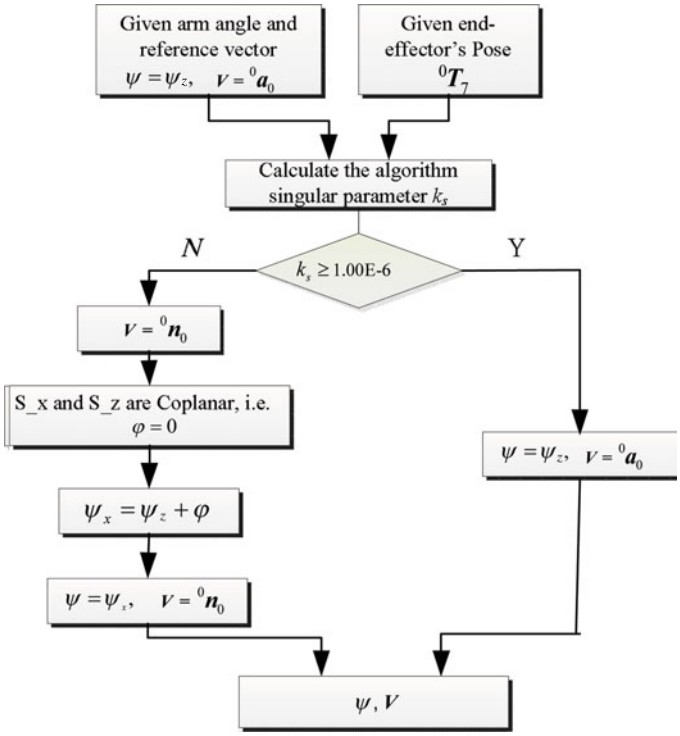

Fig. 11. Judgment of the algorithm singularity.

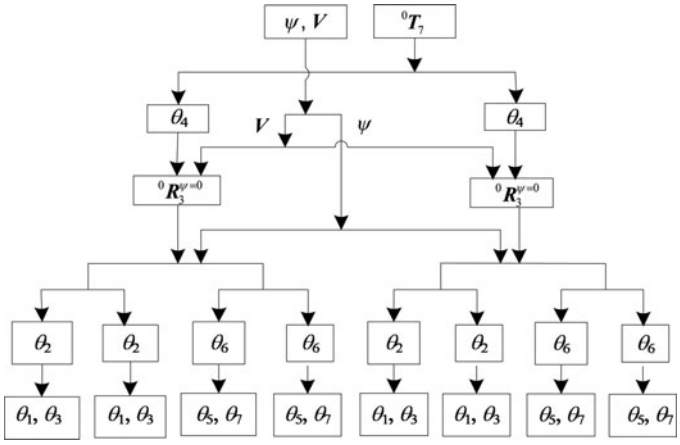

Fig. 12. Process of the arm angle parameterisation.

f) The effective reference vector $\boldsymbol{V}$ and arm angle ψ are determined. They will be used in the arm-angle parameterisation resolution, shown in Fig. 12.

The steps shown in Fig. 12 are as follows:

a) For the given pose of the end-effector ${}^0\boldsymbol{T}_7$, two solutions of the elbow joint (θ_4) are calculated using Eq. (10);
b) The absolute shoulder reference attitude matrix ${}^0\boldsymbol{R}_3^{\psi=0}$ is determined according to Eq. (47), based on θ_4 and $\boldsymbol{V}$;
c) Combining the calculated ${}^0\boldsymbol{R}_3^{\psi=0}$ with the effective ψ, the shoulder and wrist joint angles are then solved using Eqs. (19), (22) and (26).

The steps above show that there are generally eight sets of effective analytical solutions for the dual arm-angle parameterisation method.

https://doi.org/10.1017/S0263574715000284 Published online by Cambridge University Press

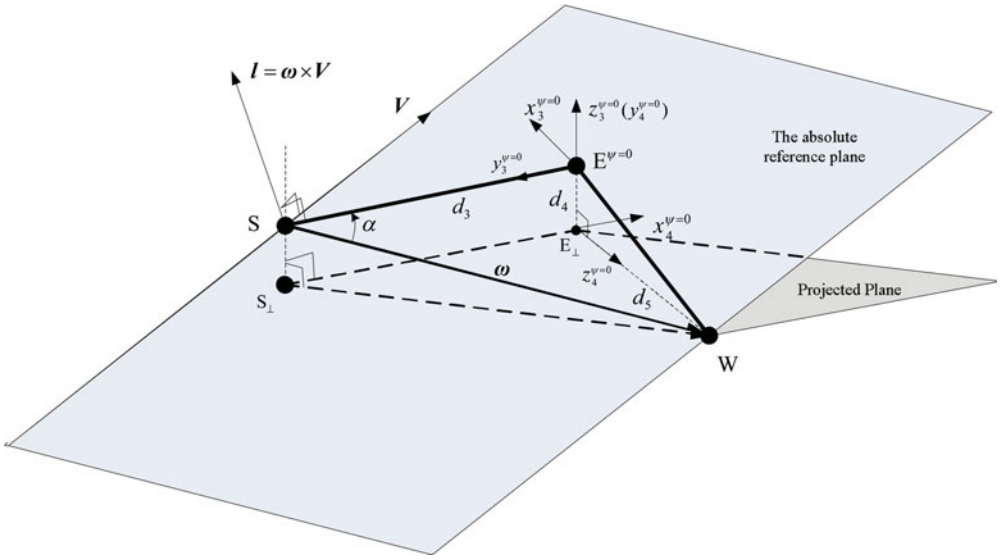

Fig. 13. Geometric relationship for $\psi = 0$.

The choice between all possible inverse kinematics resolutions is very important. The determination of a suitable solution from multiple solutions is a common problem in robotic kinematics. For real-time application, we can determine a suitable solution based on the joint limit and the current or reference configuration, as in the previous studies. We can also define three configuration flags (SHOULDER, ELBOW and WRIST) to select the appropriate solutions for the shoulder, elbow and wrist joints, respectively, as in ref. [24]. The motion planning method based on movement primitives,[25] which is based on the human arm triangle, can also be extended by use of the dual arm angle.

5. Calculation of Absolute Reference Plane and Shoulder Reference Attitude

It is obvious that the absolute reference attitude matrix ${}^0\boldsymbol{R}_3^{\psi=0}$ is very important for the solution process. However, this matrix is generally difficult to obtain and has not been supplied by the previous studies. Here, we derive the analytical expression of ${}^0\boldsymbol{R}_3^{\psi=0}$ for the case in which the pose of the end-effector is specified. The details are given below.

When $\psi = 0$, the origin of frame 3 lies in the reference plane. The relationship is shown in Fig. 13, where the symbols are defined as follows:

a) $E^{\psi=0}$ represents the elbow point when the arm plane is coplanar with the reference plane (i.e., $\psi = 0$);
b) $x_3^{\psi=0}$, $y_3^{\psi=0}$, $z_3^{\psi=0}$ represent the coordinate axes of frame 3 when the arm plane is coplanar with the reference plane (i.e., $\psi = 0$); their corresponding unit vectors are denoted by $\boldsymbol{n}_3^{\psi=0}$, $\boldsymbol{o}_3^{\psi=0}$, $\boldsymbol{a}_3^{\psi=0}$. With the upper left "0", ${}^0\boldsymbol{n}_3^{\psi=0}$, ${}^0\boldsymbol{o}_3^{\psi=0}$, ${}^0\boldsymbol{a}_3^{\psi=0}$ represent the vectors expressed in frame $\{0\}$.
c) $\boldsymbol{l} = \boldsymbol{w} \times \boldsymbol{V}$ is the unit vector orthogonal to the reference plane;
d) α is the angle from vector $\boldsymbol{w}$ to vector $\overrightarrow{SE}^{\psi=0}$.

According to the cosine law:

$$\alpha = \operatorname{acos}\left(d_3^2 + |\boldsymbol{\omega}|^2 - (d_4^2 + d_5^2)\right) / (2d_3\,|\boldsymbol{\omega}|)\,. \tag{38}$$

The vector $\boldsymbol{w}$ is collinear with $-y_3^{\psi=0}$(i.e., $-\boldsymbol{o}_3^{\psi=0}$) after rotating α around the vector $\boldsymbol{l}$:

$$\left(\boldsymbol{o}_3^{\psi=0}\right)|\boldsymbol{\omega}| = -\boldsymbol{R}\,(\boldsymbol{l}, \alpha)\cdot\boldsymbol{\omega}, \tag{39}$$

https://doi.org/10.1017/S0263574715000284 Published online by Cambridge University Press

where $\boldsymbol{R}(\boldsymbol{l},\alpha)=\boldsymbol{I}_3+\left[\boldsymbol{l}^{\times}\right]\sin(\alpha)+\left[\boldsymbol{l}^{\times}\right]^2(1-\cos(\alpha))$ and $\left[\boldsymbol{l}^{\times}\right]$ denotes the skew-symmetric matrix of the unit vector of l. Therefore, ${}^0\boldsymbol{o}_3^{\psi=0}$ is given by

$$ {}^0\boldsymbol{o}_3^{\psi=0}=-\frac{\boldsymbol{R}\left({}^0\boldsymbol{l},\alpha\right)\cdot{}^0\boldsymbol{\omega}}{\left|{}^0\boldsymbol{\omega}\right|}. \tag{40}$$

Figure 13 shows that $-d_3\boldsymbol{o}_3^{\psi=0}+d_4\boldsymbol{a}_3^{\psi=0}+d_5\boldsymbol{a}_4^{\psi=0}=\boldsymbol{\omega}$. When the vectors are described in the frame $\{0\}$, the result is as follows:

$$ -d_3\left({}^0\boldsymbol{o}_3^{\psi=0}\right)+d_4\left({}^0\boldsymbol{a}_3^{\psi=0}\right)+d_5\left({}^0\boldsymbol{a}_4^{\psi=0}\right)={}^0\boldsymbol{\omega}. \tag{41}$$

The vector ${}^0\boldsymbol{a}_4^{\psi=0}$ can also be calculated using the attitude transformation:

$$ {}^0\boldsymbol{a}_4^{\psi=0}={}^0\boldsymbol{R}_3^{\psi=0}\cdot{}^3\boldsymbol{a}_4={}^0\boldsymbol{R}_3^{\psi=0}\begin{bmatrix}s_4\\-c_4\\0\end{bmatrix}={}^0\boldsymbol{n}_3^{\psi=0}s_4-{}^0\boldsymbol{o}_3^{\psi=0}c_4. \tag{42}$$

Substituting Eq. (42) into Eq. (41) yields

$$ d_4\left({}^0\boldsymbol{a}_4^{\psi=0}\right)+d_5\left({}^0\boldsymbol{n}_3^{\psi=0}\right)s_4={}^0\boldsymbol{\omega}+(d_3+d_5c_4)\left({}^0\boldsymbol{o}_3^{\psi=0}\right). \tag{43}$$

Multiplying both sides of Eq. (43) by ${}^0\boldsymbol{o}_3^{\psi=0}$ (based on ${}^0\boldsymbol{o}_3^{\psi=0}\times{}^0\boldsymbol{a}_3^{\psi=0}={}^0\boldsymbol{n}_3^{\psi=0}$), we obtain

$$ d_4\left({}^0\boldsymbol{n}_3^{\psi=0}\right)-d_5s_4\left({}^0\boldsymbol{a}_3^{\psi=0}\right)=\left({}^0\boldsymbol{o}_3^{\psi=0}\right)\times{}^0\boldsymbol{\omega}. \tag{44}$$

Because ${}^0\boldsymbol{o}_3^{\psi=0}$ is determined according to Eq. (40), we can solve ${}^0\boldsymbol{n}_3^{\psi=0}$ and ${}^0\boldsymbol{a}_4^{\psi=0}$ by combining Eq. (43) with Eq. (44). The results are as follows:

$$ {}^0\boldsymbol{n}_3^{\psi=0}=\frac{d_5s_4\left[{}^0\boldsymbol{\omega}+(d_3+d_5c_4)\left({}^0\boldsymbol{o}_3^{\psi=0}\right)\right]+d_4\left({}^0\boldsymbol{o}_3^{\psi=0}\times{}^0\boldsymbol{\omega}\right)}{d_4^2+(d_5s_4)^2}, \tag{45}$$

$$ {}^0\boldsymbol{a}_3^{\psi=0}=\frac{d_4\left[{}^0\boldsymbol{\omega}+(d_3+d_5c_4)\left({}^0\boldsymbol{o}_3^{\psi=0}\right)\right]-d_5s_4\left({}^0\boldsymbol{o}_3^{\psi=0}\times{}^0\boldsymbol{\omega}\right)}{d_4^2+(d_5s_4)^2}. \tag{46}$$

The elbow reference attitude matrix ${}^0\boldsymbol{R}_3^{\psi=0}$ can now be determined using the three unit vectors of the x_3-, y_3- and z_3-axis, shown respectively as Eqs. (45), (40) and (46):

$$ {}^0\boldsymbol{R}_3^{\psi=0}=\left[{}^0\boldsymbol{n}_3^{\psi=0},\ {}^0\boldsymbol{o}_3^{\psi=0},\ {}^0\boldsymbol{a}_3^{\psi=0}\right]. \tag{47}$$

For the derivation above, vector $\boldsymbol{V}$ is a general symbol. It can be the unit vector of x_0, y_0, z_0 or another axis. Equation (47) is a general expression for an arbitrary reference vector.

The entire process is shown in Fig. 14.

https://doi.org/10.1017/S0263574715000284 Published online by Cambridge University Press

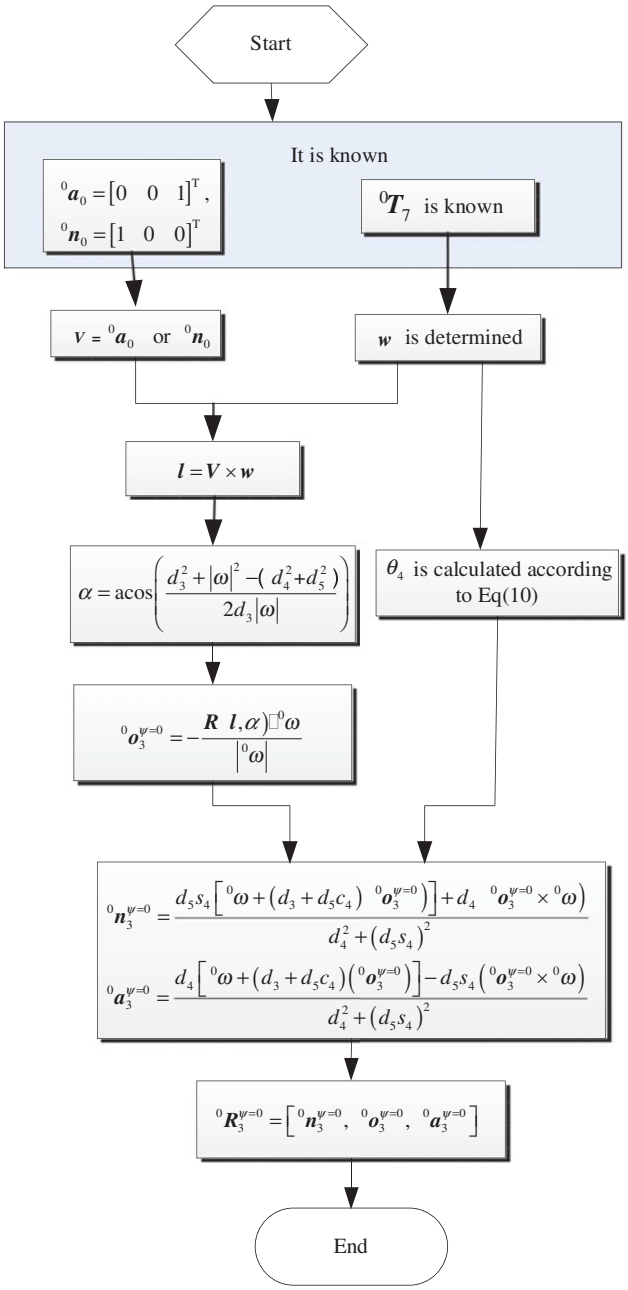

Fig. 14. Flowchart for the calculation of the shoulder reference attitude ${}^0\boldsymbol{R}_3^{\psi=0}$.

6. Case Study and Comparison Analysis

6.1. Typical cases without algorithm singularity

6.1.1. Proposed method. For a practical example, the homogeneous transformation matrix ${}^0\boldsymbol{T}_7$, representing the end-effector's pose, is assumed to be

$$ {}^0\boldsymbol{T}_7=\begin{bmatrix} 0.2468 & 0.7497 & 0.6140 & 1.4248 \\ 0.8573 & -0.4643 & 0.2223 & 0.0735 \\ 0.4517 & 0.4715 & -0.7574 & -0.3283 \\ 0 & 0 & 0 & 1 \end{bmatrix}. \tag{48}$$

https://doi.org/10.1017/S0263574715000284 Published online by Cambridge University Press

The absolute reference plane and shoulder reference attitude matrix are calculated according to the method introduced in Section 5.

First, vector ${}^0\boldsymbol{w}$ and elbow joint θ_4 are determined according to Eqs. (6) and (10), respectively:

$$ {}^0\boldsymbol{w} = {}^0\boldsymbol{P}_7 - \begin{bmatrix} 0 & 0 & d_1 \end{bmatrix}^{\mathrm{T}} - {}^0\boldsymbol{R}_7 \begin{bmatrix} 0 & 0 & d_7 \end{bmatrix}^{\mathrm{T}} = [1.2406, 0.0068, -0.4011]^{\mathrm{T}}, \tag{49} $$

$$ \theta_4 = \pi \pm \operatorname{acos}\left(\frac{d_3^2 + d_5^2 + d_4^2 - |\boldsymbol{w}|^2}{2d_3 d_5} \right) \Rightarrow \theta_4 = 5.4105 \quad \text{or} \quad \theta_4 = 0.8727. \tag{50} $$

The reference vector ${}^0\boldsymbol{V}$ is chosen to be ${}^0\boldsymbol{a}_0$. According to Eq. (37), we can obtain $k_s > 0$. The absolute reference plane is then uniquely determined by the selected reference vector $\boldsymbol{V}$ and vector ${}^0\boldsymbol{w}$. The normal vector ${}^0\boldsymbol{l}$, which is perpendicular to the reference plane, is given by

$$ {}^0\boldsymbol{l} = {}^0\boldsymbol{w} \times {}^0\boldsymbol{V} = [0.0068, -1.2406, 0]^{\mathrm{T}}. \tag{51} $$

According to Eq. (38), α is calculated as follows:

$$ \alpha = \operatorname{acos}\left(\frac{d_3^2 + |\boldsymbol{\omega}|^2 - (d_4^2 + d_5^2)}{2d_3\,|\boldsymbol{\omega}|} \right) = 0.4907. \tag{52} $$

Substituting Eqs. (49), (51) and (52) to Eq. (40), we can obtain

$$ {}^0\boldsymbol{o}_3^{\psi=0} = -\frac{\boldsymbol{R}\left({}^0\boldsymbol{l}, \alpha\right) \cdot {}^0\boldsymbol{\omega}}{\left|{}^0\boldsymbol{\omega}\right|} = [-0.6942, \quad -0.0038, \quad 0.7198]^{\mathrm{T}}. \tag{53} $$

Thus, the other two vectors, $\boldsymbol{n}_3^{\psi=0}$ and $\boldsymbol{a}_3^{\psi=0}$, are deduced by substituting Eqs. (50) and (53) into Eqs. (45) and (46). Corresponding to the two solutions of the elbow joint angle θ_4, we can obtain two shoulder reference attitude matrices as follows:

$$ {}^0\boldsymbol{R}_3^{\psi=0} = \begin{bmatrix} -0.6254 & -0.6942 & -0.3562 \\ -0.4917 & -0.0038 & 0.8708 \\ -0.6059 & 0.7198 & -0.3390 \end{bmatrix} \quad \text{for} \quad \theta_4 = 5.4105, \tag{54} $$

$$ {}^0\boldsymbol{R}_3^{\psi=0} = \begin{bmatrix} 0.6308 & -0.6942 & -0.3466 \\ -0.4848 & -0.0038 & -0.8746 \\ 0.6059 & 0.7198 & -0.3390 \end{bmatrix} \quad \text{for} \quad \theta_4 = 0.8727. \tag{55} $$

The geometric relationship of the two cases of the shoulder in the absolute reference plane is shown in Fig. 15.

It is obvious that the proposed method can be used to calculate the absolute reference plane and the shoulder reference attitude without any assumptions. It is dependent only on the given end-effector pose ${}^0\boldsymbol{T}_7$ and a selected reference vector $\boldsymbol{V}$.

For a given arm angle ψ, the corresponding joint angles are determined with the method proposed above. Due to limitations in the length of this paper, two typical cases, $\psi = 0^\circ$ and $\psi = 60^\circ$, are taken as examples.

There are eight solutions for each case. The results are listed in Tables II and III, respectively. All of the solutions are verified using the forwards kinematics in Eq. (4) by comparing the calculated ${}^0\boldsymbol{T}_7$ and that given by Eq. (48). It should be pointed out that all of the joint angles are mapped to $(-180^\circ, 180^\circ)$.

6.1.2. Comparison with the previous method. In the previous method,[21] Shimizu and Kakuya used a relative reference plane determined by setting $\theta_3 = 0^\circ$. With the constraint $\theta_3 = 0^\circ$, the seven-DOF redundant manipulator is degraded to a six-DOF PUMA-type manipulator. There are eight sets of

https://doi.org/10.1017/S0263574715000284 Published online by Cambridge University Press

Table II. Joint angles when $\psi = 0^\circ$.

I	θ_1	θ_2	θ_3	θ_4	θ_5	θ_6	θ_7
1	0.31	43.97	150.77	−50.00	17.77	49.36	136.90
2	0.31	43.97	150.77	−50.00	−162.23	−49.36	−43.10
3	−179.69	−43.97	− 29.23	−50.00	17.77	49.36	136.90
4	−179.69	−43.97	− 29.23	−50.00	−162.23	−49.36	−43.10
5	0.31	43.97	29.23	50.00	−170.07	60.82	84.33
6	0.31	43.97	29.23	50.00	9.93	−60.82	−95.67
7	−179.69	−43.97	−150.77	50.00	−170.07	60.82	84.33
8	−179.69	−43.97	−150.77	50.00	9.93	−60.82	−95.67

Table III. Joint angles when $\psi = 60^\circ$.

i	θ_1	θ_2	θ_3	θ_4	θ_5	θ_6	θ_7
1	28.34	60.29	−137.66	−50.00	−19.63	62.61	107.91
2	28.34	60.29	−137.66	−50.00	160.37	−62.61	−72.09
3	−151.66	−60.29	42.34	−50.00	−19.63	62.61	107.91
4	−151.66	−60.29	42.34	−50.00	160.37	−62.61	−72.09
5	28.34	60.29	100.79	50.00	153.01	43.74	57.09
6	28.34	60.29	100.79	50.00	−26.99	−43.74	−122.91
7	−151.82	−60.29	−79.21	50.00	153.01	43.74	57.09
8	−151.82	−60.29	−79.21	50.00	−26.99	−43.74	−122.91

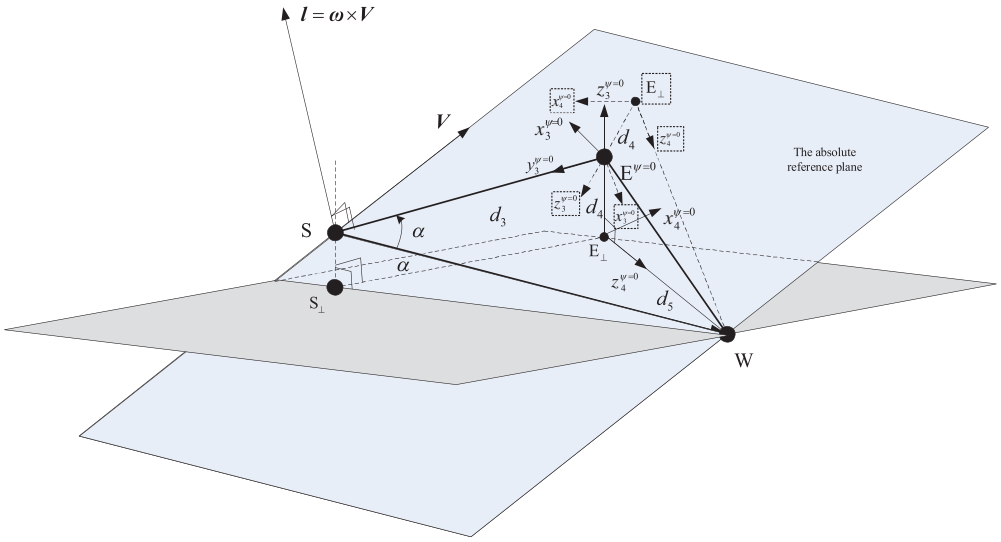

Fig. 15. Geometric relationship of two cases of the shoulder in the absolute reference plane.

solutions for the virtual non-redundant manipulator for a given ${}^0\boldsymbol{T}_7$. An arm plane formed by one of the eight solutions is then selected as the relative reference plane. The relative reference attitude is then represented as ${}^0_{\text{rel}}\boldsymbol{R}^0_3$.

For the same ${}^0\boldsymbol{T}_7$ given in Eq. (48), the eight solutions for $\theta_3 = 0^\circ$ are calculated and listed in Table IV. The relative shoulder reference attitude ${}^0_{\text{rel}}\boldsymbol{R}^0_3$ corresponding to each solution is also calculated. An angle (denoted as ψ_0) exists between the relative reference plane and the absolute reference plane defined in Section 5. The relationship is shown in Fig. 16.

For the eight solutions, ψ_0 is calculated and listed in Table IV. We can see that there are four possible cases for the relative plane and shoulder reference attitude. The previous method did not supply an absolute, uniquely determined reference plane. It is therefore not intuitive or convenient for practical application, especially the configuration control.

https://doi.org/10.1017/S0263574715000284 Published online by Cambridge University Press

Table IV. Eight solutions for $\theta_3 = 0^\circ$.

i	θ_1	θ_2	θ_3	θ_4	θ_5	θ_6	θ_7	ψ_0	${}^0_{\text{rel}}\boldsymbol{R}^0_3$
1	−13.68	96.57	0	−50.00	−115.99	23.69	45.10	−149.35	$\begin{bmatrix} -0.11 & -0.97 & -0.24 \\ 0.03 & 0.23 & -0.97 \\ 0.99 & -0.11 & 0.00 \end{bmatrix}$
2	−13.68	96.57	0	−50.00	64.01	−23.69	−134.90	−149.35	
3	−165.69	−46.57	0	−50.00	4.40	56.02	127.07	21.88	$\begin{bmatrix} -0.67 & -0.70 & -0.25 \\ -0.17 & -0.18 & 0.97 \\ -0.73 & 0.69 & 0.00 \end{bmatrix}$
4	−165.69	−46.57	0	−50.00	−175.60	−56.02	−52.93	21.88	
5	−13.68	46.57	0	50.00	−156.09	63.02	95.70	−21.88	$\begin{bmatrix} 0.67 & -0.71 & -0.24 \\ -0.16 & 0.17 & -0.97 \\ 0.73 & 0.69 & 0.00 \end{bmatrix}$
6	−13.68	46.57	0	50.00	23.91	−63.02	−84.30	−21.88	
7	−165.69	−96.57	0	50.00	31.64	6.97	98.08	149.35	$\begin{bmatrix} 0.11 & -0.96 & -0.25 \\ 0.03 & -0.25 & -0.97 \\ -0.99 & -0.11 & 0.00 \end{bmatrix}$
8	−165.69	−96.57	0	50.00	−148.36	−6.97	−81.92	149.35	

Table V. All possible solutions when $\psi_{\text{rel}} = 60^\circ$.

i	θ_1	θ_2	θ_3	θ_4	θ_5	θ_6	θ_7
1	−29.05	73.95	52.67	−50.00	94.04	10.74	143.34
2	−29.05	73.95	52.67	−50.00	−85.96	−10.74	−36.66
3	150.95	−73.95	−127.33	−50.00	94.04	10.74	143.34
4	150.95	−73.95	−127.33	−50.00	−85.96	−10.74	−36.66

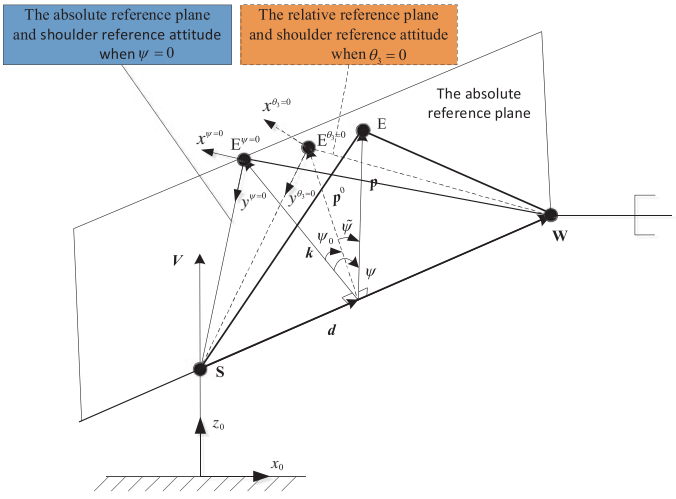

Fig. 16. References established in two ways.

Only four solutions can be obtained by the previous method. Assuming that ${}^0_{\text{rel}}\boldsymbol{R}^0_3$ is calculated according to the first solution in Table IV and $\psi_{\text{rel}} = 60^\circ$, all of the possible joint angles are calculated and listed in Table V. The solution is incomplete because the previous method only deals with one condition for θ_4. Therefore, another four sets of solutions corresponding to the other value of θ_4 cannot be determined in this manner.

https://doi.org/10.1017/S0263574715000284 Published online by Cambridge University Press

Table VI. Joint angles without algorithm singularity.

i	θ_1	θ_2	θ_3	θ_4	θ_5	θ_6	θ_7
1	130.00	164.11	129.03	−20.33	161.94	32.98	−26.58
2	130.00	164.11	129.03	−20.33	−18.06	−32.98	153.42
3	−50.00	−164.11	−50.97	−20.33	161.94	32.98	−26.58
4	−50.00	−164.11	−50.97	−20.33	−18.06	−32.98	153.42
5	130.00	164.11	50.97	20.33	−125.45	62.88	−13.51
6	130.00	164.11	50.97	20.33	54.55	−62.88	166.49
7	−50.00	−164.11	−129.03	20.33	−125.45	62.88	−13.51
8	−50.00	−164.11	−129.03	20.33	54.55	−62.88	166.49

6.2. Algorithm singularity avoidance

6.2.1. The proposed method. Let the pose of the end effector ${}^0\boldsymbol{T}_7$ be

$$ {}^0\boldsymbol{T}_7 = \begin{bmatrix} -0.5940 & 0.6806 & -0.4290 & -0.1287 \\ -0.3835 & -0.7083 & -0.5926 & -0.1778 \\ -0.7072 & -0.1875 & 0.6817 & 1.9148 \\ 0 & 0 & 0 & 1 \end{bmatrix}. \tag{56} $$

Using ${}^0\boldsymbol{T}_7$ given by Eq. (56), the position of the wrist point W is calculated and is found on the z_0-axis. If we solve the inverse kinematics using the traditional method based on a single arm angle, algorithm singularity occurs and no feasible solutions are determined.

When the vectors w and z_0-axis are coincident, an arbitrary plane containing the z_0-axis can be considered the reference plane S_z. For convenience, we can choose the plane determined by the z_0-axis and the x_0-axis as the reference plane. Then $\varphi = 0$ and $\psi_z = \psi_x$.

Taking $\psi_x = -50^\circ$ as the example, there are still eight sets of solutions for the given pose of the end-effector. They are listed in Table VI.

6.2.2. Comparison with the previous method. For the end-effector pose ${}^0\boldsymbol{T}_7$ given in Eq. (56), algorithm singularity will occur if the previous method is used. This kind of algorithm singularity appears when the end-effector pose ${}^0\boldsymbol{T}_7$ is out of the workspace of the degenerated six-DOF manipulator. The shoulder reference attitude cannot be calculated; hence, the arm-angle parameterisation cannot be realised.

From the above examples, it is obvious that our proposed method is more general than the previous method.

7. Conclusions

A class of redundant manipulators whose joints are arranged as an S-R-S structure are widely used as anthropomorphic manipulators to perform tasks that require dexterity. Because of their redundant joint, there are infinite resolutions of the position-level inverse kinematics for a specified end-effector pose. To obtain the closed-form resolution, a certain parameter must be defined to represent the redundancy. The arm angle is the most effective parameter and has been shown to be equivalent to the redundancy of the manipulator. However, the existing algorithm singularity or lack of an absolute reference plane restricts the practical applications. To overcome the shortcomings of the previous methods while retaining the advantages of the arm angle, we propose the dual arm-angle parameterisation method. Two orthogonal vectors are chosen as the reference vectors. Two corresponding reference planes are constructed, and two arm angles that satisfy a certain condition are then determined. Because there will be always at least a reasonable reference plane and an arm angle, algorithm singularity is avoided. Moreover, both reference planes are absolute reference planes. Hence, the arm angles can be used for configuration control. In addition, we supplied the analytical expressions to calculate the absolute elbow reference attitude independent of the configuration of the virtual non-redundant manipulator obtained by locking $\theta_3 = 0$. In the future, the dual arm-angle parameterisation method will be extended to other types of redundant manipulators, including those

https://doi.org/10.1017/S0263574715000284 Published online by Cambridge University Press

with more than seven joints. Subjects for further study include configuration control and redundancy resolution based on dual arm angles for arm motion analysis and real-time control.

Acknowledgements
This work was supported in part by the National Natural Science Foundation of China (61175098, 51205078) and the Basic Research Program of Shenzhen (JCYJ20140417172417095, JCYJ20130329153437293, JCYJ20140417172417129).

References

1. E. Yoshida, C. Esteves, I. Belousov, J. P. Laumond, T. Sakaguchi and K. Yokoi, "Planning 3D collision-free dynamic robotic motion through iterative reshaping," *IEEE Trans. Robot.* **24**(5), 1186–1198 (2008).
2. K. Yoshida, R. Kurazume and Y. Umetani, "Torque optimisation control in space robots with a redundant arm," *Proceedings of the IEEE/RSJ International Workshop on Intelligent Robots and Systems*, Osaka, Japan, (1991) pp. 1647–1652.
3. K. M. Ben-Gharbia, "Kinematic design of redundant robotic manipulators for spatial positioning that are optimally fault tolerant," *IEEE Trans. Robot.* **29**(5), 1300–1307 (2013).
4. H. Abdi, S. Nahavandi, Y. Frayman and A. A. Maciejewski, "Optimal mapping of joint faults into healthy joint velocity space for fault-tolerant redundant manipulators," *Robotica* **30**(4), 635–648 (2012).
5. K. A. O Neil, Y. C. Cheng and J. Seng, "Removing singularities of resolved motion rate control of mechanisms, including self-motion," *IEEE Trans. Robot. Autom.* **13**(5), 741–751 (1997).
6. K. Li and Y. Zhang, "State adjustment of redundant robot manipulator based on quadratic programming," *Robotica* **30**(3), 477–489 (2012).
7. S. Cocuzza, I. Pretto and S. Debei, "Novel reaction control techniques for redundant space manipulators: Theory and simulated microgravity tests," *Acta Astronaut.* **68**(11–12), 1712–1721 (2011).
8. J. Angeles and F. C. Park, "Performance Evaluation and Design Criteria," **In**: *Springer Handbook of Robotics* (Chapter 10), (B. Siciliano and O. Khatib, eds.) (Springer-Verlag, 2008) pp. 229–244.
9. S. Chiaverini, G. Oriolo and I. D. Walker, "Kinematically Redundant Manipulators," **In**: *Springer Handbook of Robotics* (Chapter 11), (B. Siciliano and O. Khatib, eds.) (Springer-Verlag, 2008) pp. 245–268.
10. E. Coleshill, L. Oshinowo, R. Rembala, B. Bina, D. Rey and S. Sindelar, "Dextre: Improving maintenance operations on the international space station," *Acta Astronaut.* **64**(9–10), 869–874 (2009).
11. R. Boumans and C. Heemskerk, "European robotic arm for the international space station," *Robot. Auton. Syst.* **23**(1–2), 17–27 (1998).
12. S. B. Nokleby, "Singularity analysis of the canadarm2," *Mech. Mach. Theory* **42**(4), 442–454 (2007).
13. S. Haddadin, A. Albu-Schäffer and G. Hirzinger, "Requirements for safe robots: Measurements, analysis and new insights," *Int. J. Robot. Res.* **28**(11–12), 1507–1527 (2009).
14. R. Boudreau and R. P. Podhorodeski, "Singularity analysis of a kinematically simple class of 7-jointed revolute manipulators," *Trans. Canadian Soc. Mech. Eng.* **34**(1), 105–117 (2010).
15. J. F. Soechting and M. Flanders, "Evaluating an integrated musculoskeletal model of the human arm," *J. Neurophysiol.* **119**(1), 93–102 (1997).
16. D. Liu and E. Todorov, "Hierarchical Optimal Control of a 7-DOF Arm Model," *Proceedings of the IEEE Symposium on Adaptive Dynamic Programming and Reinforcement Learning*, Nashville, TN, (2009) pp. 50–57.
17. S. Lee and A. K. Bejczy, "Redundant arm kinematic control based on parameterisation," *Proceedings of the IEEE Intemational Conference on Robotics and Autmaticm*, Sacramento, California, (1991) pp. 458–465.
18. H. Moradi and S. Lee, "Joint limit analysis and elbow movement minimisation for redundant manipulators using closed form method," **In**: *Advances in Intelligent Computing*, vol. 3645, (Berlin: Springer, 2005) pp. 423–432.
19. T. Asfour and R. Dillmann, "Human-Like Motion of a Humanoid Robot Arm Based on a Closed-Form Solution of the Inverse Kinematics Problem," *Proceedings of the IEEE/RSJ International Conference on Intelligent Robots and Systems*, Las Vegas, Nevada, (2003) pp. 1407–1412.
20. B. Tondu, "A Closed-form Inverse Kinematic Modelling of a 7R Anthropomorphic Upper Limb based on a Joint Parametrisation," *Proceedings of the IEEE-RAS International Conference on Humanoid Robots*, Genova, (2006) pp. 390–397.
21. M. Shimizu, H. Kakuya, W. Yoon, K. Kitagaki and K. Kosuge, "Analytical inverse kinematic computation for 7-DOF redundant manipulators with joint limits and its application to redundancy resolution," *IEEE Trans. Robot.* **24**(5), 1131–1142 (2008).
22. K. Kreutz-Delgado, M. Long and H. Seraji, "Kinematic analysis of 7-DOF manipulators," *Int. J. Robot. Res.* **11**(5), 469–481 (1992).
23. H. Seraji, M. K. Long and T. S. Lee, "Motion control of 7-DOF arms: The configuration control approach," *IEEE Trans. Robot. Autom.* **9**(2), 125–139 (1993).
24. W. Xu, Y. She and Y. Xu, "Analytical and semi-analytical inverse kinematics of SSRMS-type manipulators with single joint locked failure," *Acta Astronaut.* **105**(1), 201–217 (2014).
25. X. Ding and C. Fang, "A novel method of motion planning for an anthropomorphic arm based on movement primitives," *IEEE/ASME Trans. Mechatronics* **18**(2), 624–636 (2013).